Scripta-Ingenia

Matemática: beleza e harmonia, utilidade?

Titanium ring with Euler's identity, two grooves, and raw silk finish. Produced by Exotica, Exotica Jewelry and TitaniumRingsForever.com

Na recensão de José Carlos Santos, publicada na Gazeta de Matemática (nº154, 2008, pp. 30–34), sobre o livro Apologia de um matemático, de G. H. Hardy, pode ler-se que a Apologia de um matemático é a tradução para português do livro A mathematician's apology, de Godfrey Harold Hardy (1887–1947), originalmente publicado em 1940. [...]

Para Hardy, todo o valor de um resultado matemático é interno à própria matemática, ou seja, é independente das suas eventuais aplicações. Ou, nas palavras de Hardy, «não é possível justificar a vida de qualquer matemático profissional genuíno com base na 'utilidade' do seu trabalho». E como se determina o valor de um trabalho matemático? Parte da resposta está contida numa das frases mais citadas do livro:

> A beleza é o primeiro teste:
> não há lugar perene no mundo para matemática feia.

É muitas vezes referida esta visão de Hardy da inutilidade da matemática pura e do baixo apreço que tem pelas suas aplicações. Mas deve-se realçar que Hardy tem esta visão não só da matemática mas, mais geralmente, da actividade científica em geral. Por exemplo, ele escreve:

É [...] espantoso verificar o escasso valor prático que o conhecimento científico tem para as pessoas comuns, o carácter enfadonho e banal do que o tem, e como o seu valor parece variar em proporção inversa à da sua suposta utilidade.

O texto completo encontra-se em: `http://www.fc.up.pt/mp/jcsantos/Hardy.html`.

Um exemplo de beleza matemática, o qual reflecte também a sua harmonia, e apresentando talvez uma certa inutilidade, é a chamada identidade de Euler

$$e^{i\pi} + 1 = 0.$$

Nesta equação podemos encontrar cinco das constantes mais conhecidas em matemática. O número 0, elemento neutro da adição e absorvente da multiplicação, a unidade 1, elemento neutro da multiplicação, o número π, que representa a razão entre o perímetro e o diâmetro de uma circunferência, a constante e, também desiganda por número de Euler (lê-se Óiler), ou base do logaritmo natural, é o único número real positivo para o qual

$$\int_1^e \frac{1}{t} dt = 1.$$

A constante i é a unidade imaginária, não é um número real mas interage com os números reais através da relação $i^2 = -1$.

Não deixa portanto de ser extraordinário como é que estas cinco constantes, aparentemente de natureza tão distinta, se podem combinar numa única fórmula.

A Scripta-Ingenia assume-se como uma revista de divulgação científica tratando temas da ciência e da tecnologia, cobrindo todas as áreas do saber no domínio das ciências exactas ou aplicadas. Interessa-se ainda por artigos de opinião, sobre tópicos científicos ou não, desde que escritos por autores na área das ciências e da engenharia, e que reflitam as suas opiniões enquanto membros dessa comunidade. Este é o seu número sete e corresponde ao Solstício de Inverno do ano de 2016.

Director and Chief Editor — Nelson Martins-Ferreira
CDRSP-ESTG, IPLeiria

Star trail photography. Capturing the Earth's rotation.
`http://greeksky.gr/nightskyphotography/night-sky-photography-star-trails/`

A ideia de que a identidade de Euler, $e^{i\pi} + 1 = 0$, é inútil, expressa na página de rosto deste número, é, em boa verdade, apenas provocatória. Na realidade a generalização desta identidade, também conhecida por fórmula de Euler,

$$e^{i\theta} = \cos(\theta) + i\sin\theta$$

tem como consequência a importante observação de que rotação complexa, isto é, a aplicação que a cada número complexo z associa o número complexo $ze^{i\theta}$, corresponde a uma rotação no sentido anti-horário do plano complexo em torno da origem por um ângulo de θ radianos. O que claramente tem uma certa utilidade.

A Bolha de Carbono e Desenvolvimento (In)Sustentável

by CARLOS OLIVEIRA AUGUSTO

CEO da FACTOR4Sustainability e Investigador do CDRSP
E-mail: carlos.oliveira@factor4sustainability.com

Artigo de opinião

We're not going to be able to burn it all

Barak Obama, 2014

A discussão — não só fascinante, mas também relevante para o nosso futuro — respeitante à designada *Carbon Bubble* não parece estar a passar devidamente para a opinião pública, mesmo a usualmente mais bem informada.

O conceito da "Bolha de Carbono" foi introduzido pelo Carbon Tracker Iniciative, um *think-tank* dedicado à análise das consequências e riscos associados ao mercado de capitais na transição ordenada para uma economia de baixo carbono.

Neste contexto, e no pressuposto que o incremento da temperatura relacionada com o Aquecimento Global não deverá exceder +2ºC até 2050, coloca-se a questão de saber qual a quantidade de combustíveis fósseis que (ainda) poderá ser utilizada.

As estimativas apontam para um valor total de emissões derivadas da combustão de carvão, petróleo e gás natural de 2,795 $GtCO_2$, contra apenas as 565 $GtCO_2$ permitidas pelas restrições decorrentes dos compromissos internacionais assumidos, ou seja, cerca de 80% das reservas conhecidas de energia fóssil não poderão ser utilizadas (unburned), sob risco de se ultrapassar o limite estabelecido para o aumento de temperatura.

De acordo com esta perspetiva, as empresas do setor petrolífero estarão, portanto, potencialmente sobrevalorizadas em cerca de 80%, originando os chamados "ativos improdutivos" (*stranded assets*), o que representaria um risco elevado para os investidores institucionais, tais como fundos de pensões e seguradoras.
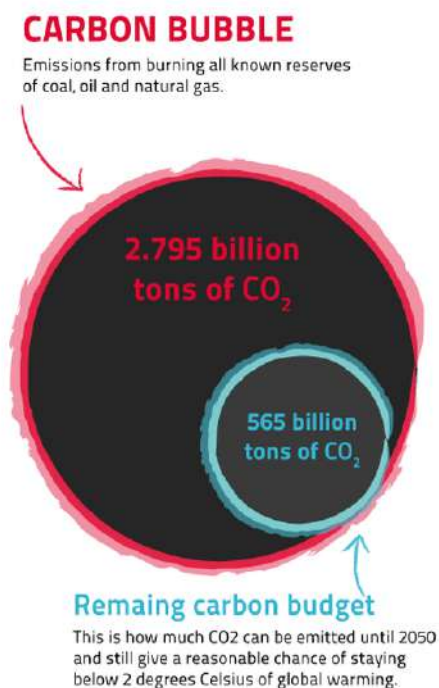
Apesar da evidência, da pressão dos investidores e da evolução tecnológica que permite atingir cada vez mais elevados patamares de eficiência para as energias renováveis, aparentemente, tudo segue igual. Parece que a "bubble" não merece a atenção devida nos *board-rooms* das multinacionais petrolíferas, tendo em conta os últimos desenvolvimentos do setor.

A Agencia Internacional de Energia (IEA) prevê um aumento de 30% da procura global de energia no período entre 2013 a 2035, sendo que a quota global estimada das energias fósseis, mantendo-se o "business as usual", será ainda de 76% no final desse período, muito por causa das necessidades energéticas das economias emergentes.

Neste cenário, o aumento previsto da temperatura global por causas antropogénicas passa a ser de 3.6ºC o que é inviável, tendo em conta o acima mencionado.

Como agir de modo a atuar de modo eficaz e atempadamente, de forma a mitigar as naturais (e catastróficas) consequências? Certamente, alinhando todas as partes interessadas de modo a desenhar uma estratégia global de mitigação das Alterações Climáticas, o que não tem necessariamente acontecido até agora.

O que nos une, como Humanidade, são as consequências devastadoras de eventos meteorológicos extremos, a destruição massiva de ecossistemas e de biodiversidade, a acidificação dos oceanos, a escassez de água e de alimentos, a educação e a pobreza materializada no facto de 2,7 mil milhões de pessoas viverem com menos de 2 USD por dia, entre outros, o que nos conduz diretamente à questão da urgente e inevitável adoção e implementação do paradigma do Desenvolvimento Sustentável.

CARBON BUBBLE

Emissions from burning all known reserves of coal, oil and natural gas.

2.795 billion tons of CO_2

565 billion tons of CO_2

Remaing carbon budget

This is how much CO2 can be emitted until 2050 and still give a reasonable chance of staying below 2 degrees Celsius of global warming.

Source: Carbon Tracker

O alinhamento de todos os *stakeholders* — empresas, instituições, ONGs, governos e cidadãos — envolvidos deve ser alcançado de modo a evitar crises ambientais,

sociais ou económicas, como também poderá ser o caso, futuramente, da *Carbon Bubble*.

No contexto atual, a "neutralização de carbono" é uma das ferramentas mais eficazes para contribuir, em simultâneo, para a satisfação das necessidades energéticas globais e para a contenção do Aquecimento Global.

De modo a obter um significativo efeito de escala, a neutralização deve, preferencialmente, ser feita a montante, a partir das empresas produtoras e distribuidoras, com o objetivo de compensar as emissões dos automóveis, empresas, organismos, escolas ou particulares.

De igual modo, estas poderão neutralizar as suas emissões de Gases com Efeito de Estufa (CO_2 equivalente) decorrentes das suas atividades, convertendo-se em empresas ou instituições "Carbon Neutral", mediante a aquisição de "Créditos de Carbono".

Desta maneira, pretende-se o seu envolvimento consciente num processo ambiental e socialmente responsável, possibilitando o financiamento de projetos de reflorestação, regeneração de solos, agricultura sustentável, e de apoio às populações através da implementação de tecnologias de biogás e de fornos solares, bem como promovendo a criação de emprego (*green jobs*) em algumas das regiões mais desfavorecidas do globo.

A estratégia de comunicação deve ser orientada para o facto de a neutralização respeitar exclusivamente às emissões de carbono que não se podem evitar, alertando ao mesmo tempo para o exemplo das boas práticas como uma oportunidade de mitigar as alterações climáticas... e de economizar.

De realçar que — de acordo com estudos levados a efeito com a colaboração do Imperial London College — a compensação efectuada com Créditos de Carbono (VCS - Verified Carbon Standards) cria significativamente mais valor (cerca de 100 vezes) do que o seu custo.

Reforestation in Kibale National Park (Uganda)
Source: Face the Future, 2017 www.facethefuture.com

Pine derived resin composites for 3-D printing

by Vidhura Mahendra and Geoffrey R. Mitchell

Centre for Rapid and Sustainable Product Development
Polytechnic Institute of Leiria
Corresponding author email: vidhura.mahendra@ipleiria.pt

Abstract Pine resins are broadly used as an adhesive material for construction applications and polycaprolactone (PCL) is a biodegradable polymer. In this work, porous pine resin-based/PCL composite scaffolds were designed and fabricated via layer by layer bio-printing, a rapid prototyping technique.
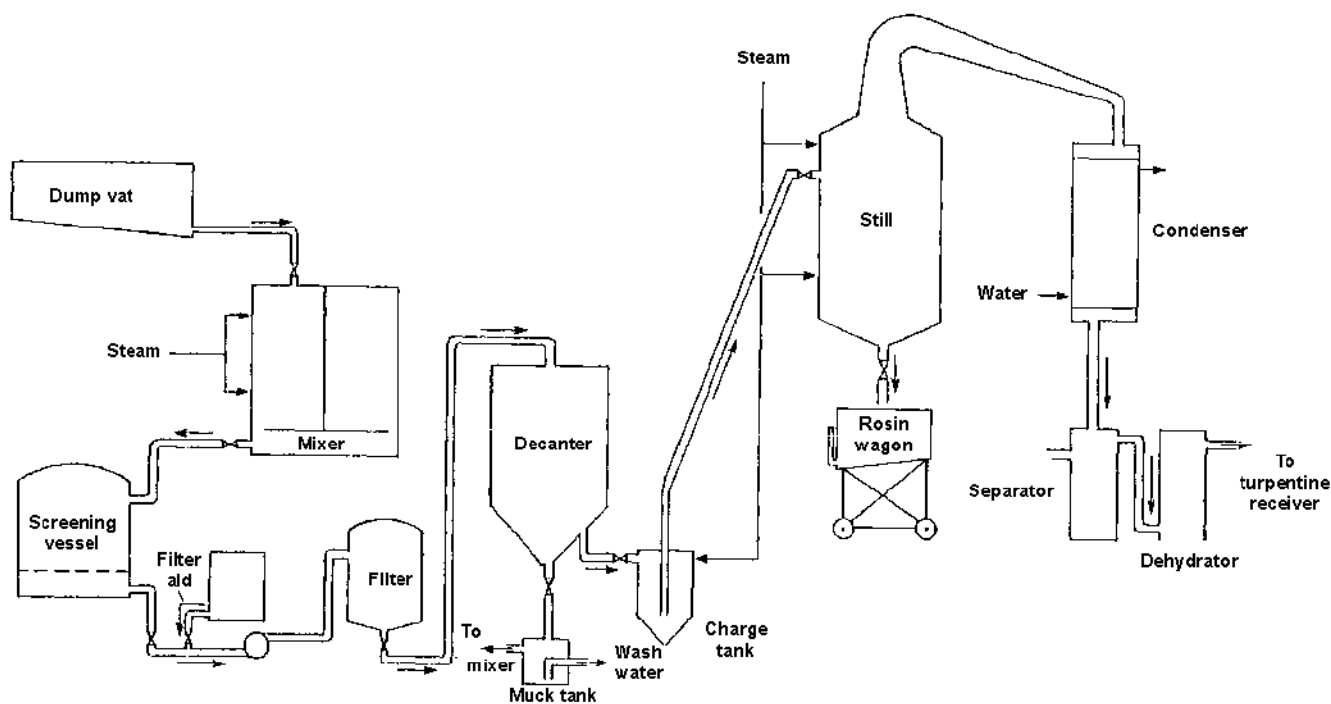
Figure 1: Separation of pine resin in to rosin, water and turpentine.

1   Introduction

Portuguese pine resins are widely known for their adhesive properties in material applications in industry [1]. Rosins are the non–volatile exudates of the pine resin which are obtained by tapping the tree and evaporating the volatile product (turpentine) collecting as flakes or sleets in a large tank (Figure 1). They usually appear pale yellow (Figure 3) to light brown in colour with a pleasant aromatic odour. The materials are traditionally used as lubricant products.

Rosin exists as a mixture of rosin acid (Figure 2, e.g. an abietic acid) is readily soluble in many organic solvents (e.g. ethanol, methanol, chloroform, dichloromethane and dimethyl formamide) which is a gateway for structural modification, chemical crosslinking and blending for reinforcements in terms of creating a composite material with appropriate mechanical properties.
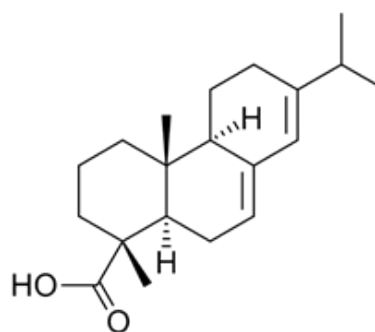

Figure 2: The chemical structure of the abietic acid, a rosin acid.

We have previously reported on fabrication of rosin composite scaffolds with nanoclay as a potential all green composite material [8].

(a)

(b)

(c)

Figure 3: The schematic route to obtaining a sample of rosin from the pine forest (a), tapping the tree (b) and obtaining the rosin (c).

2   Methodology

Gum rosins were obtained via local producers, purchased from Costa e Irmãos, Leiria, Portugal. Polycaprolactone (PCL) CAPA 6500 and chloroform were purchased from Alfa Aesar and used as they are. Experiments were conducted using standard laboratory glassware. Rosin composite scaffolds were prepared by using rosin and PCL in chloroform 10% w/v as cast films. Scaffolds were printed using a 3-D printer that can be parameterized.

The scaffolds produced were coated with gold and examined in a high vacuum Scanning Electron Microscope (Cambridge Stereoscan S360 operating at 20 kV using the secondary electron detector). The distribution of the PCl in the polymer matrix was examined using an Oxford instruments INCA system attached to the microscope which enabled maps of the elemental composition across the sample to be determined.

3   Results and Discussion

In this section we discuss the polymer blending with rosin, bio-printing ability and the structural geometry of the pine-resin based composite scaffolds.

3.1   Formation of rosin polymer blends

Rosin in polymer blends of different concentrations (Table 1) were prepared using the solvent cast method (Figure 6). Ground rosin and PCL were dissolved using chloroform in separate sample vials and once the two products were completely dissolved, mixed together and vortexed to ensure homogeneity. The blended materials were subsequently cast on Petri dishes and kept in the fume-hood for 3-4 days for solvent evaporation, alternatively can be kept in an incubator. Once the films were completely dried, removed from the Petri dishes and weighed to observe for weight loss. We have noticed that there was no weight loss and the films appeared well dispersed ensuring a satisfactory composite film (Figure 6). The films were removed from the Petri dishes, sliced in to smaller pieces for the extrusion (Figure 7) to fabricate scaffolds as desired.

Rosin (weight %)	PCL (weight %)
10	90
25	75
40	60
50	50
60	40
75	25
100	0

Table 1: Rosin and PCL concentration by weight percentage.

3.2   Bio-extrusion

The composite rosin scaffolds have been printed using the bio-extrusion system that enables the fabrication of mono and multi-material scaffolds through a layer-by-layer manufacturing process. The parameters (Table 2) were worked out to afford scaffolds that have optimum porosities (>1mm) and mechanical strengths. Rosin blend films made out of 60 and 75% were not used in printing on this occasion, however, a sample of 100% rosin was obtained for comparison purpose proved to be brittle both as a filament and scaffold (Figures 4 and 5).

We have noted the changes in the printing properties by means of not only blending rosin with a polymer in various concentrations to obtain composite scaffolds (Figure 8) but also altering the printing parameters such as the flow rate and the temperature. These changes of printing parameters ensure that naturally adhesive and brittle pine resins afforded a consistent fibre with elastic nature.

Rosin (weight %)	Extrusion Temperature (ºC)	Base plate Temperature (ºC)	Pressure (bar)	Flow rate (mm/min)	Strength of the scaffold
10	120	25	6	475	Good
25	80	15	6	650	Good
40	80	15	6	650	Good
50	80	15	6	650	Good
60	-	-	-	-	N/A
75	-	-	-	-	N/A
100	135	25	2	750	Poor

Table 2: The extrusion parameters of the rosin/rosin composite scaffolds.

Figure 4: Extruded rosin filaments at 80 ºC.

Figure 6: A solvent caste rosin composite film in a Petri dish.

Figure 5: A two-layered rosin scaffold printed at 135 ºC.

Figure 7: Sliced pieces of solvent cast rosin composite film in a Petri dish ready for bio-extrusion.
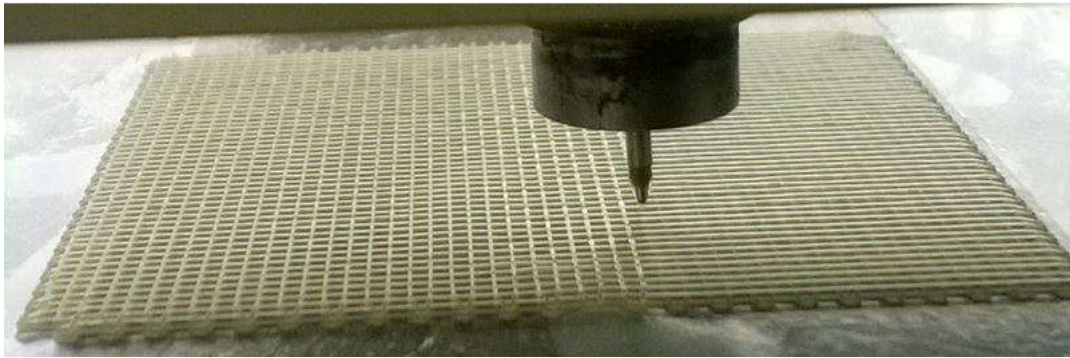
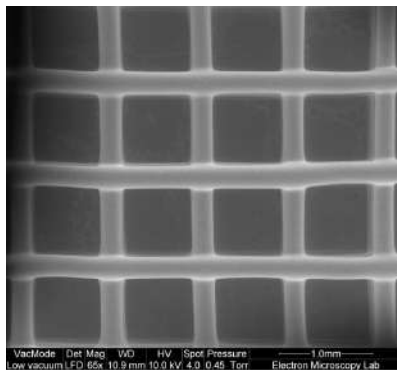*Figure 8: An example of bio-printing rosin composite scaffold of 9 layers.*

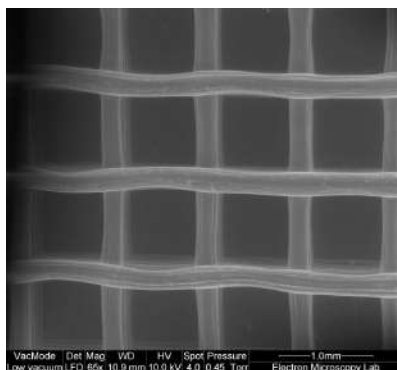*Figure 9: SEM image of the 10% rosin composite scaffold.*

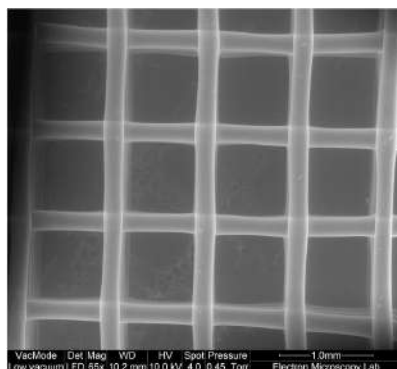*Figure 10: SEM image of the 25% rosin composite scaffold.*

Figure 11: SEM image of the 40% rosin composite scaffold.

The Scanning Electron Microscopic (SEM) images (Figures 9–11) reveal some prominent structural observations with the changes of rosin concentration in the composite scaffolds. Printing at high temperature does not show significant changes (Figure 9) at lower concentration of rosin but at high temperature shows some surface changes (Figure 10). However, printing at low temperature of high rosin concentration does not show a significant change in the scaffold (Figure 11).

4 Conclusion

Rosin composite scaffolds were produced using various concentrations in PCL. They were successfully presented in aligned fibres, good geometry and porosity. The change of printing parameters provided a steady extrusion of fibres and porosity. We expect our findings are a step forward in the advanced science and technology with related to natural product development and green chemistry.

Acknowledgement

Referências

[1] Excerpts from the book *Flavours and fragrances of plant origin*, Chapter 8, by J.J.W. Coppen, FOOD AND AGRICULTURE ORGANIZATION OF THE UNITED NATIONS, Rome, 1995.

[2] Geoffrey R. Mitchell, Sara Biscaia, Vidhura Subash Mahendra, Artur Mateus, *High Value Materials from the Forests*, Advances in Materials Physics and Chemistry, 2016, 6, 54–60.
http://dx.doi.org/10.4236/ampc.2016.63006

Movement of water molecules — a mathematical outlook

by Vidhura Mahendra and Nelson Martins-Ferreira

Centre for Rapid and Sustainable Product Development
Polytechnic Institute of Leiria
Corresponding author email: vidhura.mahendra@ipleiria.pt

Abstract A mathematical model is being considered within the context of the movement of water molecules in space. It aims to identify the three different phases in terms of their position in space and it is related with the hydrogen bonding effect.

> *Water is H$_2$O, hydrogen two parts, oxygen one, but there is also a third thing, that makes it water. And nobody knows what it is. The atom locks up two energies, but it is a third thing present which makes it an atom.*
>
> — D H Lawrence, *The third thing*,
> The works of D H Lawrence (1994), 428

1 Introduction

Water is an essential component in human life. It can occur in all three states, solid (ice), liquid and gas also known as vapour. Solid phase is the ice as in frozen water. When water freezes, its molecules move farther apart and arranges in hexagonal shapes (Figure 1), making ice less dense than water in liquid state. This means that ice will be lighter than the same volume of water and so ice will float in water. Water freezes at 0º C. Liquid water is wet and fluidic and is the phase of water with which human life most familiar with. Upon boiling (100º C) the water changes from a liquid to a gas or water vapour. As some of the water vapour cools and appears as a small cloud called steam.
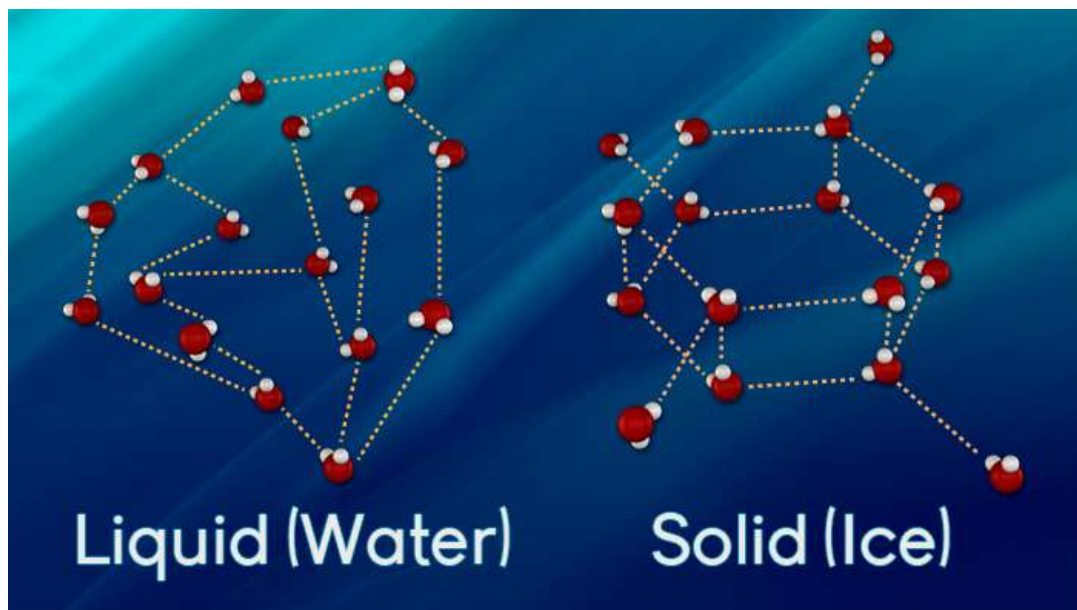

Figure 1: Liquid and Solid Water Molecules Ice is less dense than water because frozen water molecules are locked together in a fairly open network by rigid hydrogen bonds. .

2 Molecular structure and reactivity of water

Water is structurally a tiny bent molecule with the molecular formula H2O consisting of two hydrogen atoms attached to a heavier oxygen atom. Each molecule is electrically neutral but polar with the centre of positive and negative charges located in different places. Each hydrogen atom has a nucleus consisting of a single positively-charged proton surrounded by a 'cloud' of a single negatively-charged electron and the oxygen atom has a nucleus consisting of a eight positively-charged protons and eight uncharged neutrons surrounded by a 'cloud' of an eight negatively-charged electrons. On forming the molecule (Figure 2), the ten electrons pair up

into 'orbitals' one pair closely associated with the oxygen atom (known as s orbital), two pairs associated with the oxygen atom as 'outer' electrons and two pairs forming each of the two identical Oxygen-Hydrogen covalent bonds (known as p orbital).
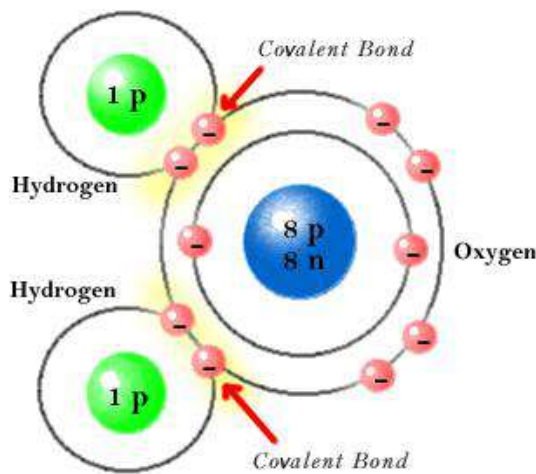
Figure 2: sp3 hybridisation of water molecule.

The other two pairs of electrons represent the so-called 'lone pairs'. These electron pairs form electron 'clouds' that are spread out approximately tetrahedrally around the oxygen nucleus as they repel each other. This is the reason for water's bent structure. The eight positive charges in the oxygen nucleus attract all these electrons strongly relative to the single positive charges on each of the hydrogen atoms. This leaves the hydrogen atoms partially devoid of electrons hence partially positively charged and the oxygen atom partially negatively charged.
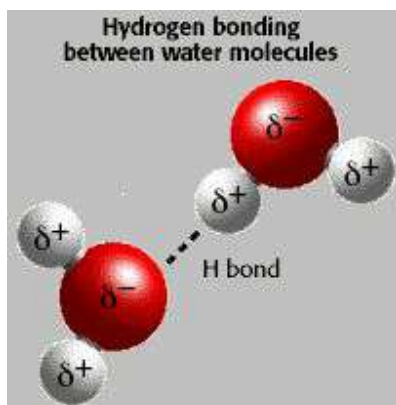

Figure 3: Hydrogen bonding takes place in water molecules between partially negatively charged Oxygen atom and partially positively charged Hydrogen atom.

Now let's see some key points in the movement of the water molecule upon heating increases the speed of the molecules. An increase in the speed of the molecules competes with the attraction between molecules and

causes molecules to move a little further apart. Cooling decreases the speed of the molecules. A decrease in the speed of the molecules allows the attractions between molecules to bring them a little closer together.

Heating a substance increases molecular motion. Cooling a substance decreases molecular motion. As molecular motion increases, the space between molecules increases. As molecular motion decreases, the space between molecules decreases.

Hydrogen bonding between water molecules is known as intermolecular forces and covalent bonding between hydrogen and oxygen is known as intramolecular forces.

3 Mathematical Model

In this section we propose a mathematical model which can be used to explain the three different states at which water can be found in our planet. We assume to have arbitrary precision tools that measure the position of atoms. Consider a parallelepiped container of 18 mm length for its base and with sufficient height to be independent of pressure. Alternatively we may consider a cubic container with length L for each side, where L is the necessary length to guarantee that one mole of water molecules is kept at constant pressure. For example, at room temperature, we would have $L = 18$ mm (18 is the molarity of the water molecule.
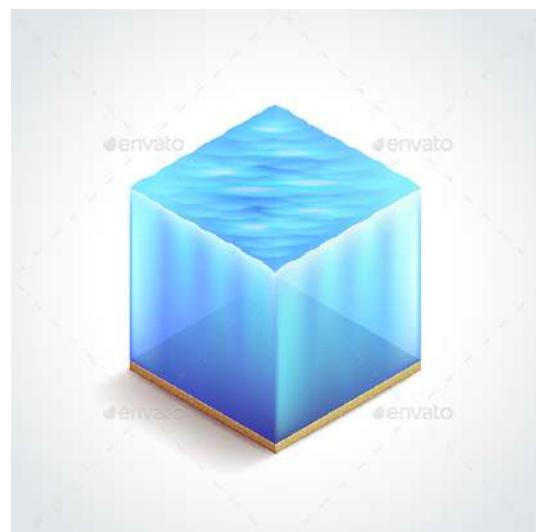

Figure 4: a water-cube [8]

Our experiment thus consists of a container with one mole of water molecules, keeping track of each of the molecules individually and explaining the variation of its states (solid, liquid and gas) as a function of temperature.

Each water molecule can be modelled as two values, λ and θ. The value λ represents the distance between the centre of the oxygen atom and the centre of each one of its hydrogen atoms (which is the same distance). The value θ is the angle between the two hydrogen atoms with respect to the oxygen atom (Figure 5).
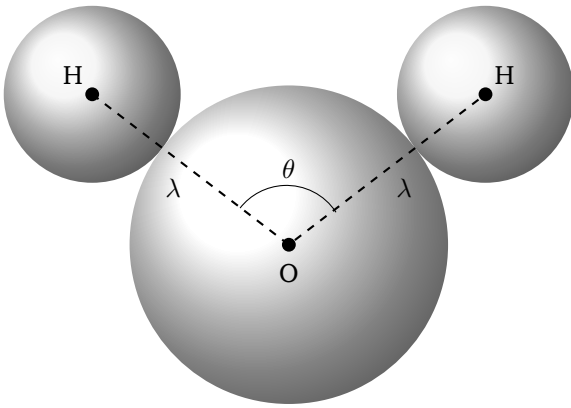
Figure 5: A water molecule with distance λ and angle θ

In order to define the model we choose one of the hydrogen atoms as first and use it as a reference. Once we have done that, we may identify a water molecule with the two values λ, θ, and represent them onto, say, the complex plane. The result is illustrated in the picture (Figure 6) representing the complex plane with the Oxygen at its origin, the first Hydrogen atom along the real axis and the second Hydrogen atom at a distance λ and an angle θ.
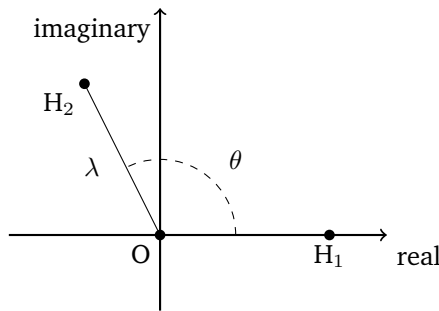

Figure 6: Axis representation of a free water molecule in space

This would mean to identify O with the zero complex number, the first hydrogen atom, H_1, with the number $\lambda = \lambda e^{i0}$ and the second hydrogen atom, H_2, with the complex number $\lambda e^{i\theta}$ (Figure 7).

In order to keep track of each individual molecule, we need to have the coordinates for the centre of the oxygen atom, (x, y, z), as well as a rotation of the three-space, which is best represented as a unit quaternion. Indeed, if $\vec{u}$ is a unit vector of $\mathbb{R}^3$ indicative of a direction of rotation, and if φ is the angle of rotation around $\vec{u}$, counter-clock wise. This information can be represented as the quaternion

$$r = cos\left(\frac{\varphi}{2}\right) + sin\left(\frac{\varphi}{2}\right)\vec{u} \qquad (3.1)$$

where we explicitly see how it encodes the rotation $\vec{u}$ and angle φ, see for example [1] for further details.

This means that every water molecule, in our system, is completely characterized by a six-tuple $(x, y, z, \lambda, \theta, r)$ where x, y, z are coordinates for the three-dimensional space, λ is a real positive number, $\theta \in [0, 2\pi[$ is an angle

and $r \in \mathbb{H}$ is a unit quaternion ($r = (r_1, r_2, r_3, r_4) \in \mathbb{R}^4$ such that $r_1^2 + r_2^2 + r_3^2 + r_4^2 = 1$). Let us now see how to realize a water molecule inside our container from the parameters $(x, y, z, \lambda, \theta, r)$ as well as how to extract the characteristic parameters from a given water molecule that is observed.

From a mathematical point of view, we can now allow ourselves to do some simplifications to the model. For an example, a water molecule, with a chosen order for its two hydrogen atoms, is mathematically a complex number $z = \lambda e^{i\theta}$. Likewise we can describe the second hydrogen atom as the complex number $\lambda e^{i\theta}$, in doing so the oxygen atom is the number $0 = 0 + 0i$ while the first hydrogen is the complex $\lambda = \lambda e^{i0} = \lambda + i0$, where $i = \sqrt{-1}$ is the imaginary unit.

In our theoretical experiment we consider one mole of molecules of water in a cubic container of length L, so that when the temperature changes, the pressure stays constant and equal to one bar.

We can now explain how to go back and forward from the mathematical model and the physical mental experience. In order to do that we need to have some general concepts on quaternion numbers ([1]).

Given a six-tuple $(x, y, z, \lambda, \theta, r)$, let us see how it positions a water molecule in the three-space. For the convenience, let us observe that from a unit quaternion r we are able to extract an angle φ and a unit vector $\vec{u}$ in $\mathbb{R}^3$, just by using the formula (3.1). The procedure to realise a water molecule is as follows: begin with the complex plane, mark the three points 0, λ, $\lambda e^{i\theta}$ on it and denote them, respectively, as O, H_1, H_2 (Figure 7).
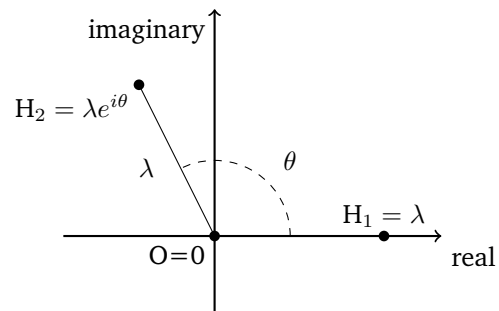

Figure 7: Representation of a free water molecule as a complex number

This first step only provides a free water molecule, we still need to position it on the three dimensional space. In order to do that we have to place the complex plane into the three dimensional space $\mathbb{R}^3$, making it parallel to the plane $y \circ z$, and matching its origin (which corresponds to $O = 0$ in the picture (Figure 7)) with the point (x, y, z). This will create a picture as illustrated (Figure 8).
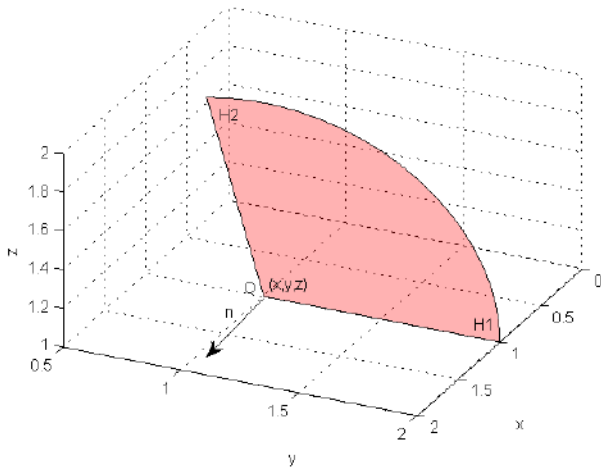
Figure 8: Placement of the complex plane onto the 3-space at a given origin (x, y, x) and normal to the vector $\vec{n} = (1, 0, 0)$. The origin of the complex plane is representing the Oxygen atom of a water molecule. The two Hydrogen atoms are also illustrated

The following step is to rotate the complex plane by the angle φ and rotate the vector $\vec{n}$ (which is parallel to the vector $(1, 0, 0)$ and perpendicular to the complex plane placed at the point (x, y, z)) so it would coincide with the vector $\vec{r}$. Figure 9 illustrates the process for a rotation of 90º around the y-axis, assuming that the origin is $O = (1, 1, 1)$, or in other words, the vector $\vec{r} = (0, 0, -1)$.
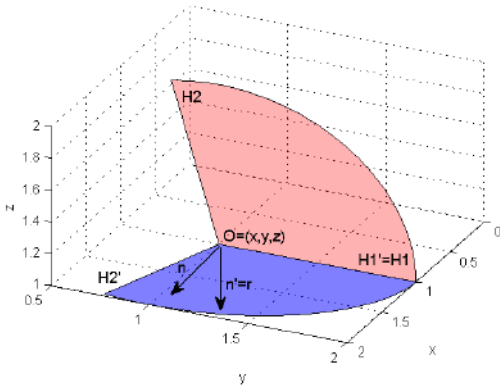

Figure 9: The process of rotating the region shown in Fig. 8 by an angle $\varphi = 0$ and a vector $\vec{r} = (0, 0, -1)$

Formally, if $T \colon \mathbb{R}^3 \to \mathbb{R}^3$ is the transformation that maps $\vec{n} = (1, 0, 0)$ into $\vec{r}$ then $H_1' = T(H_1)$ and $H_2' = T(H_2)$.

Conversely, given a water molecule in our physical system, we register the coordinates of the centre of its Oxygen atom (this gives us $O = (x, y, z)$) as well as the coordinates of the centres of the two hydrogen atoms (at this point we decide the first one of the Hydrogen atoms, as H_1, and the other as H_2). The value λ is obtained as

the distance between O and H_1, which is the same as the distance between O and H_2,

$$\lambda = \mathrm{abs}(H_1 - O) = abs(H_2 - O).$$

The angle θ is obtained as the $\arccos$ of the dot product divided by the square of the length λ,

$$\cos(\theta) = \frac{(H_1 - O) \cdot (H_2 - O)}{\lambda^2},$$

this is the usual formula to compute the angle between two vectors, in this case $\vec{OH_1}$ and $\vec{OH_2}$. It remains to explain how we can obtain the rotation angle φ and the vector $\vec{r}$. The vector $\vec{r}$ is the normal vector to the plane defined by the two vectors $\vec{OH_1}$ and $\vec{OH_2}$, and it can be obtained by the cross product

$$\vec{r} = (H_1 - O) \times (H_2 - O).$$

The angle of rotation φ is obtained by moving the vector $\vec{r}$ to match the vector $(1, 0, 0)$, which gives a transformation $T \colon \mathbb{R}^3 \to \mathbb{R}^3$ such that $T(\vec{r}) = (1, 0, 0)$, applying T to the vector $\vec{OH_1} = (H_1 - O)$, and measuring the angle that the vector $T(H_1 - O)$ does with the vector $(0, 1, 0)$, this angle is φ.

We are now ready to describe the complete model of our system for one mole of water molecules. For this purpose we need to make one more assumption, that our system evolves in time and that it is linearly dependent of the temperature. The temperature line can be illustrated (Figure 10).
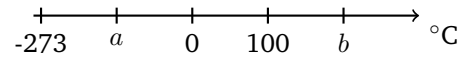

Figure 10: Temperature line with respect to a and b, the water breaking points

The values of a and b are the temperature limits upon which the water molecules break their bond and the oxygen and the two hydrogen separate themselves. At that point our formulae would not be plausible. This is to confirm that our system evolves in time and assume that the temperature is a linear function of time so that at time $t = 0$ and time $t = 100$ the temperature varies between 0ºC and 100ºC.

Under these assumptions we have that our system is described as a mapping

$$\alpha \colon A \times]a, b[\to \mathbb{R}^3 \times \mathbb{C} \times \mathbb{H}$$

whose domain is the cartesian product of the set

$$A = \{1, 2, 3, \ldots, nA\},$$

with nA representing Avogrado's number, which counts the number of atoms of Hydrogen that are contained in one gram and it is approximately 6.0221409×10^{23}, and the set

$$]a, b[= \{t \in \mathbb{R} \mid a < t < b\}$$

where a and b are the extreme values upon which (if considered as temperature values in degrees Celsius) the water molecules desintegrate, and whose codomain is the cartesian product of the euclidean 3-space, the complex numbers and the quaternions.

Each pair (i, t) in the domain, with $i = 1, 2, 3, \ldots, nA$ and $a < t < b$, is a reference to a water molecule at a given temperature and the values

$$\alpha(i, t) = (x, y, z, \lambda e^{i\theta}, r)$$

are the coordinates for the position of the water molecule.

In order to deduce the states of the water we consider a measure of the entropy of the system as follows. For each $i \in A$, at a given $t \in]a, b[$, we define

$$d_{01}(i, t) = \min_{j \in A, j \neq i}\{abs(H_1(j, t) - O(i, t))\}$$
$$d_{02}(i, t) = \min_{j \in A, j \neq i}\{abs(H_2(j, t) - O(i, t))\}$$
$$d_1(i, t) = \min_{j \in A, j \neq i}\{abs(O(j, t) - H_1(i, t))\}$$
$$d_2(i, t) = \min_{j \in A, j \neq i}\{abs(O(j, t) - H_2(i, t))\}$$

and utilise this values to obtain a measure of the total entropy in the system at a given time (temperature). This measure is given by the formula

$$\epsilon(t) = \sum_{i \in A} \frac{\min(d_{01}(i, t), d_{02}(i, t)) + d_1(i, t) + d_2(i, t)}{nA}$$

Finally, we can observe the three different states of water as a function of the temperature by plotting the entropy of the system and how it varies with temperature. We conjecture it would have a behaviour as follows, with the three different states being distinguished by way the entropy of the system varies as function of the temperature: constant=solid, linear=liquid, non-linear=gas (Figure 11).
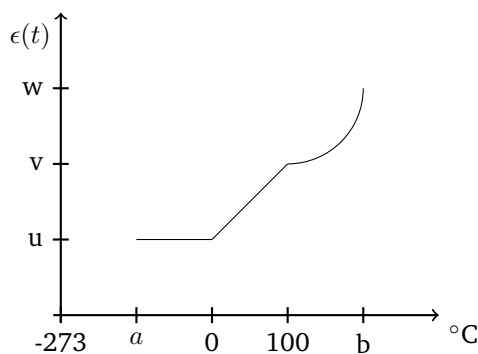

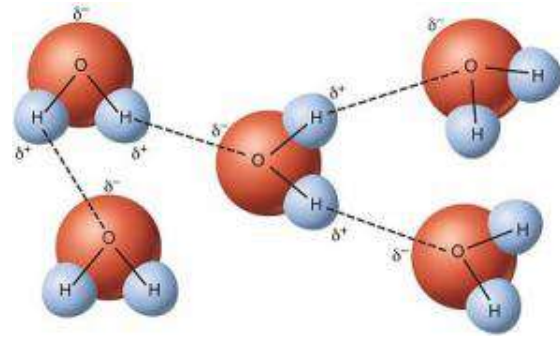*Figure 11: Possible triple-state graph of water*

Figure 12: Spacial arrangement of water molecules in terms of hydrogen bonding [9]

4 Conclusion

In this work we have attempted to provide a mathematical model in terms of the water molecular movement as a function of temperature in its tri-states (solid, liquid and gas). This can be exemplified in terms of hydrogen bonding (Figure 12) which is a rigid to weaker electrostatic force upon temperature variations on each water molecule attached with its partially negative oxygen ($O^{\delta-}$) atom to partially positive hydrogen ($H^{\delta+}$) atom at 1 atm (or 101325 Pa) pressure. The assumptions have been considered to minimise the errors and uncertainties in our system. For an example at low temperature (<0 C) the rigidity of hydrogen bonding is greater as opposed to higher temperatures thereby the movement of water molecules is greatly varied.

In a future work we will use a Brownian motion model to simulate the real movement of water molecules and compute the proposed formulas for the system's entropy. This will test the conjecture proposed for the characterization of the three states.

Acknowledgement

Referências

[1] N. Martins-Ferreira, *The quaternion algebra*, Scripta-Ingenia **4** (June) (2015) 1–2.

[2] Figure 4 credit source: https://graphicriver.net/item/isometric-water-cube-vector-illustration/11477677.

[3] Figure 12 credit source: https://manoa.hawaii.edu/exploringourfluidearth/chemical/properties-water/hydrogen-bonds-make-water-sticky

The notion of multi-link, its applications and examples

by Nelson Martins-Ferreira

Centre for Rapid and Sustainable Product Development
ESTG, Polytechnic Institute of Leiria
martins.ferreira@ipleiria.pt

Abstract In this paper we introduce the notion of a multi-link which is a new mathematical structure that can be used as a tool for the encoding and systematization of new and more efficient algorithms in the aim of 3D-printing. Applications and examples are provided.

1 Introduction

From a computer's memory storage point of view, the notion of a 2-dimensional matrix, with lines and columns, does not make much sense. At least it does not make much more sense than an arbitrarily n-dimensional matrix. In practice, what is it that it is really stored into a computer's disk memory is simply an array, and the most efficient arrays are the linear ones. In spite of everything that has been said during the last two or three decades about formal file systems, the non-structural ones are still the ones that are preferred. This explains, for example, why the STL file format is still so common nowadays.

In this paper we are proposing a new mathematical structure which on the one hand can be stored as a linear array of information, while, on the other hand, it can be used to encode highly non-trivial structures such as surfaces and their properties. These properties, as we will see, may be decomposed into logical, functional and geometrical information and they cover most of the whole spectrum of processes that are involved in 3D-printing.

The new mathematical structure that we are introducing is an abstract system, called multi-link, and it was motivated by a long series of experiments with mathematical structures and their properties, namely the ones that are related with efficiency and encoding of information. See for example [4, 2, 8, 9] and the references therein.

This work is organized as follows. We first motivate the notion of a link, which can be seen as an abstraction for the notion of a curve (appropriate for computational purposes) and then, by generalizing it into several different ways, we get the notion of multi-link. This basic notion was the result of a long period of maturation and its main characteristic is the fact that it is suitable for the encoding of n-dimensional matrices as simple linear arrays. The key ingredient is the observation that the transition maps from (i, j) to $(i + 1, j)$ and $(i, j + 1)$ can be seen as two permutable maps from the set of linearized indexes into itself. We give some details on this passage on section 3.

From section 3 onwards we concentrate our attention on the abstract notion of a multi-link by observing that it has several useful and important particular cases. Indeed, as we will see, each one of which has its purpose and can be applied into a very specific situation for 3D printing.

At he end we give a detailed description on the iso-slice algorithm, as well as an application to the generation of cooling and refrigerating channels in a mould. This will came later on, for the moment let us concentrate our attention on links, first, and then on multi-links, as a mathematical abstract structure.

2 The notion of a link and its motivation from a planar curve

A classical planar curve is usually defined as a continuous map from the unit interval $[0, 1]$ into the field of complex numbers. From the point of view of Mathematics this is a perfectly reasonable notion and it naturally extends to curves in the 3D-space. One simply substitute the field of complex numbers by the euclidean three space, and it is then just one more step to move to the n-dimensional vector field $\mathbb{R}^n$. However, from the point of view of computation, this is not really a good definition and many attempts have been made to find a better alternative. Several variations can be considered and each one of them has its own advantages and disadvantages. Here we consider one which seems to be good for the purposes of encoding contour level curves, the ones that are obtained from the slicing of triangulated surfaces, and their applications into the area of 3D-printing and direct digital manufacturing. The notion that we are proposing as an abstraction for a curve is called a link. It has arisen by observing that a curve, if approximated by a piecewise-linear sequence of directed edges, is a particular case of a directed graph. A directed graph is a mathematical object consisting in a set of vertices, a set of edges and two parallel maps that assign a vertex to an edge, namely its source and target. It turns out that some directed graphs, namely the ones that are obtained by taking an approximation to a curve, share the characteristic property of having a linking map. This linking map associates to each edge a successor edge along the direction of the curve. In this way we have arrived to the abstract notion of a link. This notion is intended to be a computational model for

a classical curve.

A link is a mathematical object which consists of a set, together with an endomap and a map into a geometrical algebra (the notion of a geometrical algebra has a precise meaning in mathematics, however, the reader not familiar with it may safely assume that it is simply a vector space, and for the purpose of this paper, $\mathbb{R}^n$ will be enough), as illustrated

$$\varphi \, \circlearrowright \, A \xrightarrow{\ g\ } \mathbb{R}^n \ .$$

This notion is thus interpreted as a generalized curve in $\mathbb{R}^n$ as follows. The curve is a piecewise linear sequence of segments; each segment in the curve is determined by an indexing element in the set of indexes A, and it is geometrically realised as the vector in $\mathbb{R}^n$ whose endpoints are

$$g(a) \longrightarrow g\varphi(a).$$

This means that each segment in the curve is indexed by an element in A, in fact we will sometimes pictured the segment as a labelled edge in a directed graph

$$g(a) \xrightarrow{\ a\ } g\varphi(a).$$

The set A is called the set of indexes, the map φ is called the successor, or transition map (it tells to each index, which is considered as the origin of the edge, what is its successor — the successor is at the same time the endpoint of its predecessor and the starting point of the edge of which it is the index of), this idea can be illustrated as follows

$$g(a) \xrightarrow{\ a\ } g\varphi(a) \xrightarrow{\varphi(a)} g\varphi^2(a) \longrightarrow \cdots$$

For further examples we refer the reader to [5].

3 Moving from an array to a matrix while keeping it linear

If we try to generalize the notion of a link as an abstraction of a curve into some new abstract entity which would serve as a good model for a surface, we would easily be led to something with the form

$$X \times Y \xrightarrow{\ \varphi\ } X \times Y \xrightarrow{\ g\ } \mathbb{R}^n \ .$$

However, as soon as we try to interpret it as a surface we soon realize that $\varphi(x,y) = (\varphi_1(x,y), \varphi_2(x,y))$ should be of the form

$$
\begin{array}{ccc}
(\varphi_1(x), y) & \longrightarrow & (\varphi_1(x), \varphi_2(y)) \\
\uparrow & & \uparrow \\
(x, y) & \longrightarrow & (x, \varphi_2(y)).
\end{array}
$$

In other words, it should consist on two independent maps $\varphi_1 \colon X \to X$ and $\varphi_2 \colon Y \to Y$, together with the realization (or geometrical) map

$$X \times Y \xrightarrow{\ g\ } \mathbb{R}^n \ .$$

The role of φ_1 and φ_2 is to determine the behaviour of the transitions along the x-direction and the y-direction. Note that these directions are only abstract and they should not be confused with the directions of $\mathbb{R}^n$.

Let us see a concrete example. Suppose we are interested in modelling the cylinder

$$C = \{(x,y,z) \in \mathbb{R}^3 \mid x^2 + y^2 = 1, \quad 0 \le z \le 1\},$$

in this case we could do an approximation, say, with $X = \{1, 2, 3, \ldots, 360\}$, $Y = \{0, 1\}$ and define the maps $\varphi_1 \colon X \to X$, $\varphi_2 \colon Y \to Y$ and $g \colon X \times Y \to \mathbb{R}^3$ as follows: $\varphi_1(x) = x + 1$ if $x < 360$ and $\varphi_1(360) = 1$; $\varphi_2(0) = \varphi_2(1) = 1$; and

$$g(u,v) = \left(\cos\left(\frac{2\pi u}{360}\right), \sin\left(\frac{2\pi u}{360}\right), v \right)$$

As already remarked at the introduction, the crucial point here is to observe that we may exchange the set $X \times Y$ with another set, which is bijective to it, say A, and the endomap $\varphi \colon X \times Y \to X \times Y$ with two endomaps $\alpha, \beta \colon A \to A$ that are permutable, i.e., $\alpha\beta = \beta\alpha$. In this way we form squares indexed by the elements of A as illustrated

$$
\begin{array}{ccc}
\beta(a) & \longrightarrow & \alpha\beta(a) \\
\uparrow & & \uparrow \\
a & \longrightarrow & \alpha(a).
\end{array}
$$

If the set X has n_X elements, and the set Y has n_Y elements, then we can take the set A to be the set $\{1, 2, 3, \ldots, n_X n_Y\}$ and the well known bijection which transforms pairs of indexes (i, j) into linear indexes $a = i n_X + j$.

The notion of a multi-link is a natural generalization of the notion of link and it is motivated by the concrete examples of a square-link (like the one above), a double-link (which is a structure that models arbitrary surfaces) and several other that where designed for more specific purposes, such as contour filling algorithms or generating voxelized porous 3-dimensional physical structures from the real world.

4 Multi-link

The notion of multi-link arises thus as a need to encode and organize the whole bunch of information in the form of data and algorithms that are used in the whole process of 3D printing in general and conceptual terms.

A multi-link is a mathematical object consisting in a set, called a set of indexes, say A, a collection of endomaps, say $\alpha_i \colon A \to A$ with $i \in \mathbb{N}$, called the transition

maps, a map, say g from the set of indexes into a geometrical algebra (again the reader not familiar with a geometrical algebra may assume that it is simply a finite dimensional vector space), this map is called the geometric realization map, and a collection of surjective maps $p_j \colon A \to B_j$ with $j \in \mathbb{N}$. The maps may be subject to some commutativity conditions written in the form of equations expressed in terms of the composition of maps. The diagram displaying all the information may be pictured as follows.

$$\alpha_i \, \begin{array}{c} \curvearrowright \end{array} A \xrightarrow{\ g\ } \mathbb{R}^n$$
$$\downarrow{\scriptstyle p_j}$$
$$B_j$$

with $i \in \{1, 2, 3, \ldots, n\}$ and $j \in \{1, 2, 3, \ldots, m\}$.

The family of maps (α_i) is considered to be the logical part of the multi-link (since it deals with the indexes and re-indexation), the map g is considered for obvious reasons to be the geometrical part, while the family of projections (p_j) is considered as the functional part of the structure. This is because in most of the examples the projection maps are simply assigning some functional behaviour to the edges, like color properties or materials or other kind of physical interpretation which in practice gives to a specific edge what its role is, in the sense of what its function is about.

let us now see some concrete examples of the structure. In the following sections we give some details on how the structures can be used as well as from where they were motivated.

4.1   Particular cases as examples

4.1.1   Coloured link

A coloured link is simply a link with a surjective map into some set C, of colors, in other words it is of the form

$$\alpha \, \begin{array}{c} \curvearrowright \end{array} A \xrightarrow{\ g\ } \mathbb{R}^n$$
$$\downarrow{\scriptstyle c}$$
$$C$$

such that $c\alpha = c$.

It is interpreted as a link in which every edge has a certain color associated to it, and moreover, the edges in the same component (in the sense of orbits of α) have the same color, but different components may have different colors.

4.1.2   A square-link

A square link was introduced above and it can be seen as a special case of a multi-link with two endomaps and no projections. Moreover the two endomaps, say α and β, have to be permutable, that is, we should have $\alpha\beta = \beta\alpha$.

If we take the example of the cylinder from above and use the bijection

$$\phi \colon X \times Y \to A$$

from the cartesian product of $X = \{1, \ldots, 360\}$ and $Y = \{0, 1\}$ into $A = \{1, \ldots, 720\}$ which is defined by $\phi(i, j) = i + j360$, then, in order to give the structure of a square-link it remains to specify the maps $\alpha, \beta \colon A \to A$ and $g \colon A \to \mathbb{R}^3$. In this case we should put $\alpha(360) = 1$, $\alpha(720) = 361$ and $\alpha(x) = x + 1$ in the other cases. For the map β we should have $\beta(x) = 360 + x$ if $x \le 360$ and $\beta(x) = x$ for all the other values of $x \in A$. The map g is now defined as

$$g(x) = \left(\cos\left(\frac{2\pi x}{360}\right), \sin\left(\frac{2\pi x}{360}\right), 0 \right)$$

when x is less or equal to 360 and

$$g(x) = \left(\cos\left(\frac{2\pi(x - 360)}{360}\right), \sin\left(\frac{2\pi(x - 360)}{360}\right), 1 \right)$$

for the cases when x is greater than 360.

4.1.3   A triangulation

The structure of a triangulation has been studied in [6] and it is an important example of a multi-link.

The structure of a triangulation generalizes the one of a directed graph. It consists of two sets (vertices and triangles) and three parallel maps between them, as displayed

$$T \begin{array}{c} \xrightarrow{a} \\[-4pt] \xrightarrow{b} \\[-4pt] \xrightarrow{c} \end{array} V. \tag{4.1}$$

An element $t \in T$ is interpreted as a triangle in the following manner
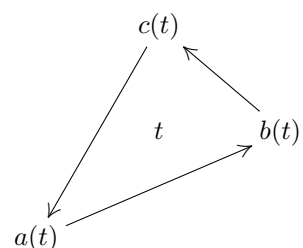

In practice we are concerned with triangulated surfaces in the three dimensional euclidean space

$$T \begin{array}{c} \xrightarrow{a} \\[-4pt] \xrightarrow{b} \\[-4pt] \xrightarrow{c} \end{array} \mathbb{R}^3, \tag{4.2}$$

In [6] we explain that those triangulations which are obtained as the boundary of a physical real object in the 3-D euclidean space are the ones with the property that every vertex has a start-neighbourhood of triangles. In other words, these triangulations are the ones for which the collection of triangles that are incident into a given

vertex can be cyclically ordered by sharing an adjacent face, as illustrated.

(4.3)
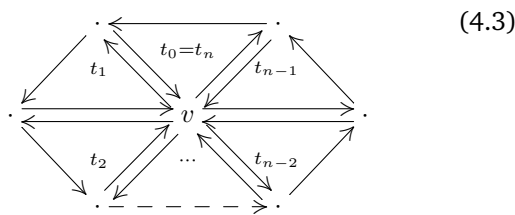
The passage from a triangulation into a multi-link is performed in [6] as a way of efficient encoding the triangulations that have the desired property, namely that all vertices have a star-neighbourhood. For practical reasons we substitute $\mathbb{R}^3$ with the Cayley algebra (or geometric algebra) of quaternions $\mathbb{H}$, see [1]. In [6] it is proved that the triangulations

$$T \underset{c}{\overset{a}{\underset{b}{\rightrightarrows}}} \mathbb{H},$$

(4.4)

in which every vertex has a star-neighbourhood, are equivalent (has a mathematical structure, in the sense that they contain the same information) to a multi-link of the form

$$\theta,\varphi \; \overset{\curvearrowleft}{\circlearrowright} A \xrightarrow{\;g\;} \mathbb{H}$$

(4.5)

such that

$$\theta^3 = 1_A$$ (4.6)
$$\theta^2 = \varphi\theta\varphi$$ (4.7)
$$g\varphi = g$$ (4.8)

and moreover, in order to have the *star-neighbourhood* property displayed in (4.3) one should add the requirement that φ is an isomorphism.

4.1.4 A double-link

The notion of a double-link encodes in the most general way the concept of a surface. Here we will only give the definition and the simple example of the tetrahedron. Further examples and the study of its main properties are postponed for future work. The examples of the other platonic solids can be found in [3].

A double-link is an instance of a multi-link which can be displayed as

$$\alpha,\beta \; \overset{\curvearrowleft}{\circlearrowright} A \xrightarrow{\;g\;} \mathbb{R}^4$$
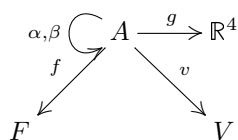
and it is such that

$$\alpha\beta\alpha\beta = 1_A$$
$$\beta\alpha\beta\alpha = 1_A$$
$$f\alpha = f$$
$$v\beta = v$$

The example of a tetrahedron, due to its simplicity, can be used to better illustrate the notion under analysis. From the following picture, which shows the planar graph representation of a tetrahedron (with the usual directed edges replaced by oriented squares that are build up from the labels α and β), we can deduce a concrete example of a double-link, as follows.
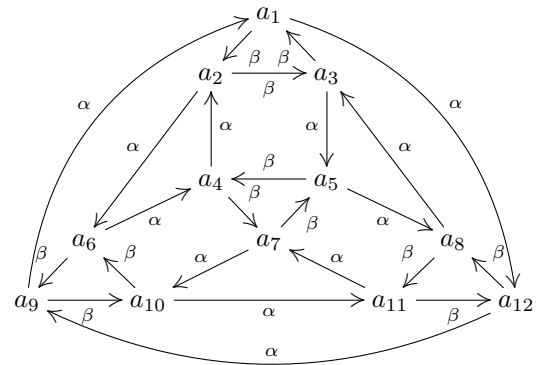
Take A to be the set $\{a_1, \ldots, a_{12}\}$ and let the endomaps α and β be defined by the labels indicated in the planar graph representation, that is $\alpha(a_1) = a_{12}$, $\beta(a_1) = a_2$, etc. The projection map f is the quotient over the orbits of α, which means it gives us the faces of the tetrahedron. The projection map v is the quotient over the orbits of β, this gives us the set of vertices. The map g can be any realization of the elements from A into a space and we omit the details of it.
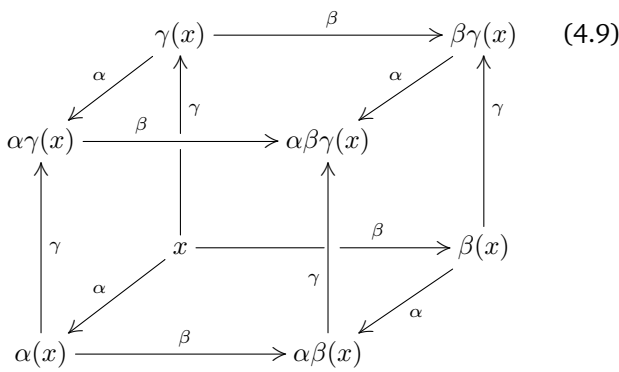
4.1.5 A cubic-link

A cubic link is a straightforward generalization of a square-link and it is useful in modelling volumes with porous structures on it, see for example the Technical Report [10] produced by the Laboratory of Topology and Geometry from CDRSP-IPLeiria.

A cubic link is a structure

$$\alpha,\beta,\gamma \; \overset{\curvearrowleft}{\circlearrowright} A \xrightarrow{\;g\;} \mathbb{H} \simeq \mathbb{R}^4$$

such that $\alpha\beta = \beta\alpha$, $\alpha\gamma = \gamma\alpha$ and $\gamma\beta = \beta\gamma$. It is interpreted as a collection of voxels of a cubic shape. In the same way as a square-link models a surface which is generated by a square patch along two abstract directions, a cubic link can be used to generate a 3d-manifold which is generated by a collection of cubes attached along three

different abstract directions, say α, β, γ, as illustrated.

$$\text{(4.9)}$$

4.1.6   A n-cube-link

Again, a straightforward generalization of a cubic-link is obtained if instead of three abstract directions we consider any finite number n and thus obtaining

$$\alpha_i \ \underset{\curvearrowright}{\bigcirc} \ A \xrightarrow{g} \mathbb{G} \ , \quad i = 1, 2, \ldots, n$$

where $\mathbb{G}$ is any geometrical algebra (or more simply a vector space), and the α_i are permutable in the sense that $\alpha_i \alpha_j = \alpha_j \alpha_i$ for any i, j in $\{1, 2, \ldots, n\}$

This structures arises for example in the construction of n-dimensional volumes with porous structures on its interior and it has some applications in 3D-printing.

4.2   A contour filling curve

The paper [7] describes a procedure on how to generate sweep trajectories for planar regions that are encoded by its boundary and obtained by slicing a three-dimensional body.
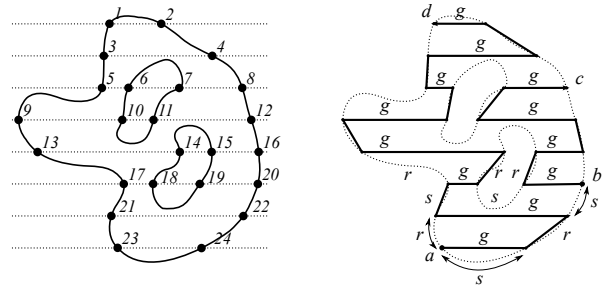
The details that are in the base of the motivation for considering this structure are referred to [7]. Here we recall the structure that is used there, which is an instance of a multi-link. It consists on a diagram of sets and maps, as illustrated,
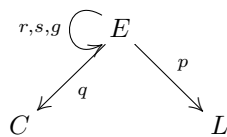
such that

$$r^2 = s^2 = g^2 = 1_E$$
$$qr = qs = q$$
$$pg = p$$

It may be illustrated as in the following pictures

where the role of the maps r, s, g is visible in the picture on the right. As we have said, our concern here is only to illustrate the structure of a multi-link with one more concrete example and its application, we refer the reader to the paper [7] for further details on this topic.

4.2.1   A square patch

A square patch is an intermediate level between a square-link and a double-link. It is the analogue to a triangulation except that it is made out of squares rather than triangles. The generalization from a triangulation is not difficult to obtain and we omit the details. As an instance of a multi-link it is described as follows.

$$\theta, \varphi \ \underset{\curvearrowright}{\bigcirc} \ A \xrightarrow{g} \mathbb{H} \tag{4.10}$$

such that

$$\theta^4 \ = \ 1_A \tag{4.11}$$
$$\theta^3 \ = \ \varphi \theta \varphi \tag{4.12}$$
$$g\varphi \ = \ g \tag{4.13}$$

The orbits of θ are now interpreted as the faces (which are all squares) while the orbits of φ are interpreted as the vertices.

5   The iso-slice algorithm

In this section we give the necessary details for an implementation of an algorithm that efficiently computes level iso-contours. The contours are the ones obtained by slicing a triangulated surface in the euclidean 3d-space with respect to an iso-surface of a given level.
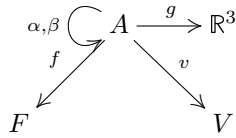
The algorithm may be decomposed in the following following steps:

(1) Consider a triangulation as input

$$T \ \overset{a}{\underset{c}{\overset{\longrightarrow}{\underset{\longrightarrow}{\overset{\longrightarrow}{b}}}}} \ V \ \overset{x}{\underset{z}{\overset{\longrightarrow}{\underset{\longrightarrow}{\overset{\longrightarrow}{y}}}}} \ \mathbb{R}$$

(2) Transform the given triangulation into a double-link as explained before (see also [6]). This gives

us a structure of the form

$$\alpha,\beta \, \overset{\curvearrowright}{} \, A \overset{g}{\longrightarrow} \mathbb{R}^3$$

$$f \swarrow \qquad \searrow v$$

$$F \qquad\qquad V$$

with the meaning that the orbits of α are the faces (elements in F) and the orbits of β are the vertices (elements in V).

(3) Suppose there is also given a family of iso-surface in the 3d-space, say defined by a map

$$F \colon \mathbb{R}^3 \to \mathbb{R}$$

which intuitively may be thought of as assigning to every point in space a certain hight; the main example is $F(x,y,z) = z$, this gives us planar slices along the z-direction, but we may also have $F(x,y,z) = x^2 + y^2$ or $F(x,y,z) = x^2 + y^2 + z^2$ and have, respectively, cylinders and spheres; arbitrary maps are possible as well and depending on each particular case of application they are defined in a specific way with a specific meaning, the algorithm, however, works for an arbitrary map.

(4) Transform the structure of double link from item 2 into the structure of a coloured link by considering $\varphi = \beta\alpha$, $h = Fg$ and forgetting the projection map v, this gives us

$$\varphi = \beta\alpha \, \overset{\curvearrowright}{} \, A \overset{h=Fg}{\longrightarrow} \mathbb{R}$$

$$f \downarrow$$

$$F$$
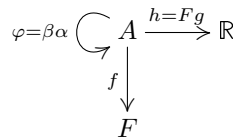
the map h is intuitively the hight of each point in A relative to the iso-surface level F from item 3;

(5) For each contour level $r \in \mathbb{R}$ do:

(a) obtain the subset of A in the coloured link from item 4 defined by:

$$A_r = \{ a \in A \mid h(a) \le r < h\varphi(a) \}$$

(b) consider the directed graph whose edges are the elements in A_r as well as the vertices; the domain map is the identity map and the codomain map is $\varphi = \beta\alpha$, this will produce a picture which may be interpreted as illustrated
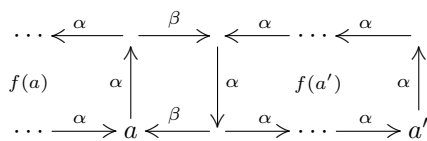
where we suppose that both a and a' are in A_r. This means that $r \in \mathbb{R}$ is a hight laying between $h(a)$ and $h\beta\alpha(a)$ as well as between $h(a')$ and $h\beta\alpha(a')$. The idea is to link a and a' and to do so it is sufficient to identify the orbits of α via f. This procedure creates a directed graph.

(c) construct the directed graph

$$A_r \overset{d}{\underset{c}{\rightrightarrows}} F$$

from the subset $L \colon A_r \hookrightarrow A$ (item 5(a)) to the set of faces F (item 4), with $d = fL$ and $c = f\varphi L = f\beta\alpha L$. This graph is obtained by applying the quotient map f to the graph considered in item 5(b).

(d) Link the digraph from 5(c), that is, find $\varphi_r \colon A_r \to A_r$ such that $d\varphi_r = c$. This is a general process and it can be performed in a unique way, provided the faces are geometrically convex. Indeed, Let $E \overset{d}{\underset{c}{\rightrightarrows}} V$ be an arbitrary directed graph, it has a symmetry, that is, there exists a bijective map $\varphi \colon E \to E$ such that $d\varphi = c$ if and only if the incoming edges are in bijection with the outcoming ones, for every vertex in V. In our case, if the faces are convex then they will either not be intersected by the iso-surface level r or they are intersected exactly in two different edges (in the picture displayed at item 5(b) this was assumed to happen at the edges starting at the indexes a and a').

(e) Construct the link structure

$$\varphi_r \, \overset{\curvearrowright}{} \, A_r \overset{g_r}{\longrightarrow} \mathbb{R}^3 \ ,$$

with $g_r(a) = g(a) + t_r(g\varphi(a) - g(a))$ where

$$t_r = \frac{r - h(a)}{h\varphi(a) - h(a)},$$

recall that $\varphi = \beta\alpha$ and $h = Fg$, come from item 4.

(6) Collect all the links structures (A_r, φ_r, g_r) for all the contours $r \in \mathbb{R}$ in which we may be interested in and return this information as output.

6   An example of application

An example of application for the iso-slicing algorithm is the following. Suppose we have a solid body object of which we want to produce a mould with refrigeration channels. This means that if $S \subseteq \mathbb{R}^3$ is our solid then we are interested in the region of the space $\bar{S} = \mathbb{R}^3 \setminus S$. Moreover, suppose we wish to make some channels along the surface area of the boundary of $\bar{S}$, while keeping the

channels on the interior of the region. Furthermore, in order to simplify the process, let us assume that these channels are generated by planar curves parallel to the xy-plane. To do so we need to determine how the ratio distance between two consecutive layers should be defined so that the cooling temperature is isotropic along the surface metric. One way to do it is to use our procedure, the iso-slice algorithm. The key aspect of it is to define the hight function $F\colon \mathbb{R}^3 \to \mathbb{R}$. In this case the high function is interpreted as the distance measured along the surface between the points in a lower level and the corresponding ones in the upper level immediately above it. We give below some details on how this procedure can be implemented.

Suppose (T, V, a, b, c, x, y, z) is a triangulation such as the one given on item 1 of section 5, which is considered to be an approximation to a surface defined by the boundary of $S = closure(interior(S)) \subseteq \mathbb{R}^3$. We are interested in generating contour levels along the iso-surfaces which are geodesics along a direction perpendicular to the xy-plane. These contour paths will give us the generators for the cooling channels. In order to do that we observe the following steps:

(1) obtain a square-link from the given triangulation:

  (a) find an appropriate set of contours equally spaced that can serve as a good approximation to the given triangulation;

  (b) for each one of the contour levels identified on the previous item, execute the slicing algorithm with $F(x, y, z) = z$;

  (c) resample the number of points obtained in each set of indexes from the final link (as in item 5(2) from section 5) so that they all have the same number of points;

  (d) construct a square-link by letting A to be the union of all A_r, assuming that we have chosen say, $r \in \{r_0, r_1, \ldots, r_n\} \subseteq \mathbb{R}$ and that each A_r has, say, $m = 100$ elements. This is done by letting the map α to be given by the collection of φ_r and β to identify each point in the level r_i with the closest one on the level r_{i+1}. This does not necessarily give a structure for a surface which is homeomorphic to the initially given one but it is equivalent from the point of view of the generation of the cooling channels.

(2) having a square link (A, α, β, g) as defined in section 4.1.2 we now define the iso-surface family $F\colon A \to \mathbb{R}$ iteratively as follows (suppose $\phi\colon A \to X \times Y$ is a bijection with $X = \{0, 1, \ldots, n\}$ and $Y = \{1, \ldots, m\}$). The base points, that is the ones in the level r_0, are all zero $F(x, 0) = 0$; all the points at the same level will have the same value under F; suppose we have $F(x, y)$ given, then we define $F(x, y + 1)$ as the formula

$$F(x, y) + \|g\phi^{-1}(x, y) - g\phi^{-1}(x, y + 1)\|$$

(3) we now use the iso-slicing algorithm with the new hight value F.

(4) the end result of this procedure gives a family of contour levels parallel to the xy-direction which are isotropic along the geodesic paths measured on the surface.

Having the contour trajectories enveloping the original surface in a way which is isotropic concerning the refrigeration distribution of heat along the geodesic distances on the surface, we can then choose a cross-section for the channels and generate the final structure as a square-patch.

7 Conclusion

All this procedures and processes have been implemented in a computer system and proved to be efficient and robust. Indeed, the fact that the data can be modelled as a mathematical structure has the great advantage that it characterizes completely the input data, the output data, as well as the abstract structures which are involved in any intermediate step in the process.

Acknowledgement

Referências

[1] N. Martins-Ferreira, *The quaternion algebra*, Scripta-Ingenia **4** (June) (2015) 1–2.

[2] M. B. Gaspar and N. Martins-Ferreira, *A procedure for computing the symmetric difference of regions defined by polygonal curves*, J. Symb. Comput. **61-62** (2014) 53–65 .

[3] M. Gaspar, M. Leite, N. Martins-Ferreira and B. N. Panda, *Computer construction of Platonic Solids*, Scripta-Ingenia **4** (June) (2015) 6–11.

[4] M. Gaspar and N. Martins-Ferreira, *Optimization of toolpath trajectories on arbitrary surfaces*, Scripta-Ingenia **3** (December) (2014) 9–13.

[5] M. Gaspar and N. Martins-Ferreira, *Finite Orbit decomposition of endomaps*, Scripta-Ingenia **3** (December) (2014) 23–26.

[6] N. Martins-Ferreira, *On the structure of a triangulation*, Scripta-Ingenia **5** (December) (2015) 22–23.

[7] M. B. Gaspar and N. Martins-Ferreira, *Continuous sweep strategies for filling arbitrary regions in the plane (Portuguese)* , Bol. Soc. Port. Mat. (Spec. Iss.) (2010) 78–86 .

[8] M. B. Gaspar and N. Martins-Ferreira, *Robust STL processing for extrusion-based manufacturing*, Innovative Developments in Virtual and Physical Prototyping, 2012 , 273-278.

[9] N. Alves, P. Bartolo, N. Martins-Ferreira, M. B. Gaspar and A. Mateus, *BioFab toolbox Software tools for biofabrication*, High Value Manufacturing: Advanced Research in Virtual and Rapid Prototyping, 2013, 483-487.

[10] Nelson Martins Ferreira, Tim Woodfield and Khoon Lim, *A tool for the generation of 3D-voxelized-mesh-grid gyroid surfaces in the aim of SkelGen*, CDRSP-IPLeiria Technical Report, GTLab(SkelGen-2) **71** (2016).

University of Cape Town, South Africa